Lipids (2016) 51:549–560
DOI 10.1007/s11745-015-4117-6

ORIGINAL ARTICLE

Mouse Strain Impacts Fatty Acid Uptake and Trafficking in Liver, Heart, and Brain: A Comparison of C57BL/6 and Swiss Webster Mice

D. R. Seeger[1] · E. J. Murphy[1]

Received: 28 July 2015 / Accepted: 10 December 2015 / Published online: 21 January 2016

Abstract C57BL/6 and Swiss Webster mice are used to study lipid metabolism, although differences in fatty acid uptake between these strains have not been reported. Using a steady state kinetic model, [1-^{14}C]16:0, [1-^{14}C]20:4n-6, or [1-^{14}C]22:6n-3 was infused into awake, adult male mice and uptake into liver, heart, and brain determined. The integrated area of [1-^{14}C]20:4n-6 in plasma was significantly increased in C57BL/6 mice, but [1-^{14}C]16:0 and [1-^{14}C]22:6n-3 were not different between groups. In heart, uptake of [1-^{14}C]20:4n-6 was increased 1.7-fold in C57BL/6 mice. However, trafficking of [1-^{14}C]22:6n-3 into the organic fraction of heart was significantly decreased 33 % in C57BL/6 mice. Although there were limited differences in fatty acid tracer trafficking in liver or brain, [1-^{14}C]16:0 incorporation into liver neutral lipids was decreased 18 % in C57BL/6 mice. In heart, the amount of [1-^{14}C]16:0 and [1-^{14}C]22:6n-3 incorporated into total phospholipids were decreased 45 and 49 %, respectively, in C57BL/6 mice. This was accounted for by a 53 and 37 % decrease in [1-^{14}C]16:0 and 44 and 52 % decrease in [1-^{14}C]22:6n-3 entering ethanolamine glycerophospholipids and choline glycerophospholipids, respectively. In contrast, there was a significant increase in [1-^{14}C]20:4n-6 esterification into all heart phospholipids of C57BL/6 mice. Although changes in uptake were limited to heart, several significant differences were found in fatty acid trafficking into heart, liver, and brain phospholipids. In summary, our data demonstrates differences in tissue fatty acid uptake and trafficking between mouse strains is an important consideration when carrying out fatty acid metabolic studies.

Keywords Heart · Lipid metabolism · Palmitic acid · Arachidonic acid · Docosahexaenoic acid · Fatty acid uptake · Fatty acid trafficking

Abbreviations

SW	Swiss Webster
TAG	Triacylglycerol(s)
FFA	Free fatty acids
DAG	Diacylglycerol(s)
Ptd_2Gro	Cardiolipin
EtnGpl	Ethanolamine glycerophospholipids
PtsIns	Phosphatidylinositol
PtdSer	Phosphatidylserine
ChoGpl	Choline glycerophospholipids
CerPCho	Sphingomyelin
16:0	Palmitic acid
20:4n-6	Arachidonic acid
22:6n-3	Docosahexaenoic acid
Acox1	Acyl-CoA oxidase 1
FABP	Fatty acid binding protein

Introduction

Both C57BL/6 and Swiss Webster (SW) mice have been extensively used for decades as general purpose model for research and drug safety testing. Interestingly, there are several strains of Swiss Webster outbred mice sold by various breeders, which over time, these mice may have acquired slight genetic drift despite their common origin. In contrast, C57BL/6 mice are the most widely used inbred strain due to its permissive background for maximal

✉ E. J. Murphy
eric.murphy@med.und.edu

[1] Department of Basic Sciences, School of Medicine and Health Sciences, University of North Dakota, 501 N Columbia Road, Room 1701, Grand Forks, ND 58203-9037, USA

expression of most mutations. Although there are several breeder specific strains available, due to this mouse being an inbred strain, it generally has less genetic drift between commercial sources than SW mice. Genetic variations between mouse strains are important and have been shown to affect phenotype. Therefore, we are interested in differences between tissue uptake and trafficking of fatty acids in these two commonly used strains.

Metabolism is significantly affected by mouse strain differences. Several studies support the hypothesis that different strain variants have an effect on phenotype. Despite similar insulin sensitivity and secretion in several inbred strains, C57BL/6 mice are the least glucose tolerant of mice studied [1, 2]. However, conflicting glucose tolerance data was found when C57BL/6 mice are fed a high-fat diet and compared to a different 129 substrain, 129T2 compared to 129X1, suggesting that differences in strains used to compare to C57BL/6 mice can affect data interpretation [3]. Furthermore, C57BL/6 mice subjected to a high-fat diet have increased body fat mass and decreased oxygen consumption, coupled with lower endurance capacity and decreased β-oxidation in the liver, which correlates to increased obesity compared to other inbred strains [4, 5]. These data suggest liver and muscle metabolism differences contribute to physical performance and susceptibility to diet-induced obesity.

Interestingly, substrain differences in lipid metabolism in C57BL/6J compared to C57BL/6N mice have also been observed, with a high-fat diet inducing an increase in plasma insulin and blood glucose in the C57BL/6N substrain, resulting in more severe hepatic steatosis and inflammation [6]. Similar results are found in an *ob*/*ob* obesity model in inbred strains of C57BL/6 mice which more rapidly cleared circulating triacylglycerol (TAG), resulting in a more severe hepatic steatosis [7]. Another study comparing C57BL/6 substrains found a functional deletion in the nicotinamide nucleotide transhydrogenase gene in C57BL/6J mice [8]. Similarly, a study in 129 substrains found genetic variations have a considerable impact on strategies that involve targeted mutagenesis [9]. These data support the observation that studies between strains cannot be treated interchangeably without mention of genetic variations that could contribute to alterations in interpretation of results.

SW and C57BL/6 mice are extensively used for the study of lipid metabolism. Brain- and heart-fatty acid binding protein (FABP) were isolated from the brain of SW mice [10], while C57BL/6 mice are often used to study n-3 lipid metabolism and its potential benefits after ischemia and spinal cord injury [11–13] Further, hearts of C57BL/6 mice have decreased incorporation of exogenous radiolabeled oleic acid as compared to several other inbred strains as a result of increased mRNA expression of acyl-CoA oxidase 1 (*Acox1*) [14]. Interestingly, several inbred and outbred mouse strains including C57BL/6 and CD-1:SW have a mutation in the gene encoding for secretory group II phospholipase A_2, with C57BL/6 mice having a homozygous frameshift mutation in the $sPLA_2$ gene, while CD-1:SW mice were heterozygous for this same mutation [15]. However, what impact mouse strain has on tissue fatty acid uptake and trafficking into specific lipid pools is unknown.

To address this gap in knowledge, we determined the impact of strain differences in fatty acid uptake and trafficking in SW and C57BL/6 mouse strains using a steady-state radiotracer kinetic model [16, 17]. Strain influences on [1-^{14}C]16:0, [1-^{14}C]20:4n-6, or [1-^{14}C]22:6n-3 uptake and trafficking in liver, heart, and brain *in vivo* was determined. These data show for the first time, that mouse strain impacts whole body 20:4n-6 metabolism as indicated by increased radiotracer in plasma in C57BL/6 mice as compared to SW mice. We also found an increased incorporation and trafficking of [1-^{14}C]20:4n-6 in a number of heart phospholipids of C57BL/6 mice. Further in heart, the decreased incorporation of [1-^{14}C]16:0 and [1-^{14}C]22:6n-3 into the total phospholipid pool was accounted for by a profound reduction in esterification into the ethanolamine glycerophospholipids (EtnGpl) and choline glycerophospholipids (ChoGpl) in C57BL/6 as compared to SW mice. From these data we conclude that there are significant differences in lipid metabolism mainly in heart between these mice, which suggests that genetic background plays a substantial role in fatty acid trafficking.

Methods

Surgery and Fatty Acid Infusion

Samples were collected from 3 month old Swiss Webster and C57BL/6 male mice (National Institute of Cancer, Frederick, MD, USA) under an approved protocol by the University of North Dakota (Grand Forks, ND, USA) Animal Care and Use Committee (protocol 0110-1). During catheter insertion mice were anesthetized with (1–3 %) Halothane and polyethylene10 catheters were inserted into the right femoral vein and artery. Mice were allowed to recover from anesthesia for three hours following surgery to allow equilibration of metabolism [18, 19]. After recovery, mice were infused with 170 μCi/kg of either [1-^{14}C]16:0, [1-^{14}C]20:4n-6, or [1-^{14}C]22:6n-3 at a rate of 50 μl/min for 10 min to achieve steady state plasma radioactivity. Blood was collected at set intervals and plasma separated to assess intravascular radioactivity. Mice were then euthanized at 10 min with pentobarbital (i.v.) and immediately subjected to head focused microwave irradiation to heat denature enzymes *in situ* [17, 20]. Whole brain, liver, and heart were removed, flash frozen in liquid

nitrogen, and then pulverized into a homogeneous powder under liquid nitrogen conditions. Because of the contribution of residual blood to tissue radioactivity, whole blood was extracted using a two-phase extraction method [21] as previously described [22]. Residual blood in liver, heart, and brain was estimated to be 17, 22, and 2 %, respectively, based upon previously published data [23–26].

Tissue Lipid Extraction

Following pulverization, lipids were extracted from the tissues using a two-phase extraction method [21]. Powdered tissue was kept on dry ice until added to a tared Tenbroeck homogenizer, to determine the mass (g ww) of the tissue added. To the Tenbroeck homogenizer 17 vol. of chloroform and methanol (2:1, by vol) was added. Once tissue was homogenized, the extract was removed, saved and then the homogenizer was washed with 3 vol. of chloroform and methanol (2:1, by vol) and the rinse added to the initial extract. The tissue residue was saved for protein quantification. After homogenization, 4 vol of 0.9 % KCl was added to extract, mixed by vortexing, and allowed to separate into two phases overnight at −20 °C under a $N_{2(g)}$ atmosphere. The following morning, the top phase was removed and saved. To the lower phase, 4 vol. of chloroform, methanol, and water (3:48:47, by vol) was added, the sample vortexed, chilled, and subjected to centrifugation to facilitate phase separation. The upper phase was removed and combined with the previous upper phase to determine aqueous fraction radioactivity using liquid scintillation counting (LSC). The lower phase was dried down with N_2 (g) and dissolved in hexane:2-propanol (3:2, by vol) and a portion used to determine organic radioactivity using LSC. The unused portion was stored under N_2 (g) atmosphere at −80 °C in hexane:2-propanol (3:2, by vol).

Lipid Separation by Thin Layer Chromatography

Extracted lipids were separated using thin layer chromatography (TLC) on heat-activated (110 °C) Whatman silica gel-60 plates. Neutral lipids were separated into individual classes using petroleum either, diethyl ether, and acetic acid (75:25:1.3, by vol.) [27]. Phospholipids were separated into individual classes using chloroform, methanol, acetic acid, and water (50:37.5:3:2, by vol.) [28]. Lipids were visualized using iodine (phospholipids) or 6-(*p*-toluidino)-2-naphthalenesulfonic acid (TNS) (neutral lipids) and identified using commercially available standards (Avanti, Polar Lipids, Alabaster, AL, USA). Once lipids were visualized, the silica was scraped into glass scintillation vials and 0.5 mL ddH_2O was added to facilitate desorption of lipids from the silica. Then 10 mL of Scintiverse BD cocktail (Fisher Scientific, Pittsburgh, PA, USA) was added and samples were mixed by vortexing and then allowed to settle for 1 h. Samples were counted on a Beckman LS 6500 liquid scintillation counter equipped with low-level detection software (Fullerton, CA, USA).

Protein Quantification

Protein content in the tissue residue was quantified using a modified dye-binding assay utilizing bovine serum albumin as a standard [29]. The tissue residue was dried of residual solvent and then subjected to hydrolysis with 0.2 KOH at 65 °C overnight [30]. Samples were then mixed with dye binding reagent and allowed to equilibrate for 10 min prior to reading on a spectrophotometer at 595 nm.

Statistics

Statistical analysis was done using the Instat® statistical program (Graphpad, San Diego, CA). Multiple comparisons were assessed using a one-way ANOVA with a Tukey–Kramer *post hoc* test, with $p < 0.05$ considered as significant, $n = 3$–4. A two-tailed Student's t test was used to determine significance between treatment groups, with $p < 0.05$ considered to be significant, $n = 3$–4.

Results

Plasma Area Under the Curve was Significantly Different for [1-^{14}C]20:4n-6 Infusions

The effect of strain differences on fatty acid tracer content in plasma in SW and C57BL/6 mice was determined by incremental plasma sampling during the steady state radiotracer infusion. The tracer content in plasma is vital for the calculation of the coefficient of incorporation, k_i*, where radioactivity in a given compartment is divided by the integrated area under the curve for plasma radioactivity for each individual mouse. There was a significant difference ($p < 0.05$) in plasma curve area, 1334 ± 100 ($n = 4$) for C57BL/6 and 1024 ± 121 ($n = 4$) for SW mice (Fig. 1). Plasma areas for [1-^{14}C]16:0, 945 ± 80 (C57BL/6) *versus* 925 ± 85 (SW) and for [1-^{14}C]22:6n-3, 1212 ± 75 (C57BL/6) *versus* 1154 ± 91 (SW), were not significantly different between strains (Fig. 1). The reduced [1-^{14}C]20:4n-6 tracer concentration in plasma of SW mice could be a result of enhanced uptake of 20:4n-6 into tissues in these mice as compared to C57BL/6.

C57BL/6 Mice Have Increased Total Uptake into Heart Tissue

Tissue fatty acid uptake and incorporation into the organic and aqueous fractions was determined (Table 1). In heart,

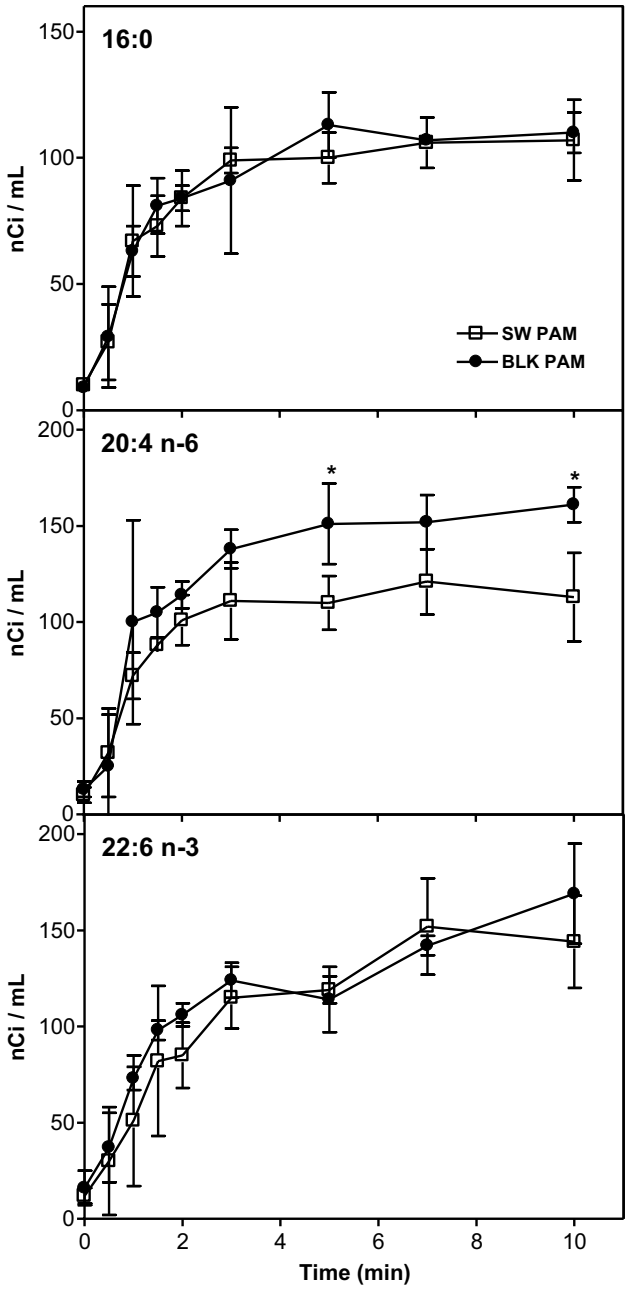

Fig. 1 Plasma curves for [1-^{14}C]16:0, [1-^{14}C]20:4n-6, and [1-^{14}C]22:6n-3 comparing infusion of radiotracer fatty acids into SW and C57BL/6J mice. SW (*unfilled box*) and C57BL/6 (*filled circle*) were infused with [1-^{14}C]16:0 (*upper panel*), [1-^{14}C]20:4n-6 (*middle panel*), and [1-^{14}C]22:6n-3 (*lower panel*). Values are expressed as nCi/mL as found in plasma collected during radiotracer infusion and represent mean ± SD ($n = 3$–4). The *asterisk* indicates a statistically significant difference from SW and C57BL/6 strains using one-way ANOVA and a Tukey–Kramer *post hoc* test was used for plasma curves and a Student's *t* test was used to compare the area under the curve between strains ($p < 0.05$)

there was a significant 1.7-fold increase in total uptake of [1-^{14}C]20:4n-6, accounted for by a 1.8-fold increase in incorporation into the organic fraction of C57BL/6 mice (Table 1). Although, the total uptake of [1-^{14}C]22:6n-3 into heart was not significantly different, the incorporation into the organic fraction was reduced 33 % in C57Bl/6 compared to SW mice (Table 1). There was no difference in [1-^{14}C]16:0 total uptake or in incorporation into organic or aqueous fractions. For all of the fatty acid tracers, there was no significant difference in the heart aqueous fraction, which represents products of β-oxidation [18, 31, 32].

Liver and brain tissue did not have significant differences in uptake or incorporation into organic or aqueous fractions, suggesting the observed differences between strains were specific to [1-^{14}C]20:4n-6 uptake into heart tissue and incorporation of [1-^{14}C]22:6n-3 into the organic fraction.

Metabolic Targeting into Phospholipid and Neutral Lipid Pools are Differentially Modulated in Heart

Phospholipid and neutral lipid fractions were separated to determine fatty acid targeting differences in SW and C57BL/6 mice (Table 2). For liver, [1-^{14}C]16:0, uptake into neutral lipids decreased 18 % in C57BL/6 mice (Table 2), but no other changes were observed. In heart, there was a significant reduction in the incorporation of [1-^{14}C]16:0 (45 %) and of [1-^{14}C]22:6n-3 (49 %) into phospholipids in C57BL/6 compared to SW mice (Table 2). Furthermore, C57BL/6 mice have decreased [1-^{14}C]16:0 (45 %) fractional distribution into heart phospholipids (Table 2). In contrast, incorporation of [1-^{14}C]20:4n-6 into C57BL/6 heart phospholipids increased 2.2-fold compared to SW mice (Table 2). We observed no difference in 20:4n-6 and 22:6n-3 trafficking into heart neutral lipids between groups (Table 2). There were no significant changes in [1-^{14}C]16:0, [1-^{14}C]20:4n-6, or [1-^{14}C]22:6n-3 fatty acid tracer uptake or trafficking in brain (Table 2). These data indicate that mouse strain impacts specific tissue fatty acid uptake and trafficking and predominately impacts targeting into phospholipids in the heart.

Strain Specific Differences in Fatty Acid Targeting into Individual Lipid Classes

To determine fatty acid targeting into individual lipid classes in SW and C57BL/6 mice, phospholipid and neutral lipid fractions were separated. In liver there was a significant 17 % decrease in [1-^{14}C]16:0 incorporation into

Table 1 Distribution of fatty acid tracer into liver, heart, or brain organic and aqueous fractions in SW and C57BL/6 mice

	$k^* \times 10^{-5}$ (s^{-1})				Fractional dist. (%)			
	SW		C57BL/6		SW		C57BL/6	
	Mean	STD	Mean	STD	Mean	STD	Mean	STD
16:0								
Liver								
Org	1010	156	842	83	85	13	85	8
Aq	172	27	145	19	15	2	15	2
Total	1182	183	988	102				
Heart								
Org	166	44	166	30	40	11	39	7
Aq	245	29	259	21	60	7	61	5
Total	411	73	425	51				
Brain								
Org	19	5	14	7	47	14	44	22
Aq	21	1	18	2	53	3	56	7
Total	40	7	32	9				
20:4n-6								
Liver								
Org	804	166	727	205	80	17	77	22
Aq	199	49	221	28	20	5	23	3
Total	1003	215	948	234				
Heart								
Org	379	101	679	156*	72	19	76	17
Aq	145	17	217	67	28	3	24	8
Total	524	118	895	223*				
Brain								
Org	26	7	24	4	65	18	61	10
Aq	14	2	15	2	35	4	39	5
Total	40	9	39	6				
22:6n-3								
Liver								
Org	644	258	603	198	76	31	75	25
Aq	198	50	200	48	24	6	25	6
Total	842	309	803	246				
Heart								
Org	422	78	284	48*	81	15	77	13
Aq	96	32	84	15	19	6	23	4
Total	518	110	368	63				
Brain								
Org	29	13	20	7	78	36	71	26
Aq	8	2	9	1	22	4	29	5
Total	37	15	29	9				

Distribution of [1-^{14} C]16:0, [1-^{14}C]20:4n-6, or [1-^{14}C]22:6n-3 tracer into organic and aqueous fractions of liver, heart, and brain. Values represent means ± SD ($n = 3$–4). The asterisk indicates a statistically significant difference between SW and C57BL/6 strains using a Student's unpaired, two-tailed t test ($p < 0.05$)

Org organic fraction, *Aq* aqueous fraction

triacylglycerol pools (TAG) (Table 3), consistent with the reduction observed in the neutral lipid fraction of C57BL/6 mice compared to SW mice (Table 2). A 1.2-fold increase in esterification of [1-^{14}C]20:4n-6 into EtnGpl was found in liver but, there were no differences in esterification of [1-^{14}C]22:6n-3 into liver between strains (Table 3).

Table 2 Incorporation of fatty acid tracer into liver, heart, or brain phospholipid and neutral lipid pools in SW and C57BL/6 mice

	$k^* \times 10^{-5}$ (s^{-1})				Fractional dist. (%)			
	SW		C57BL/6		SW		C57BL/6	
	Mean	STD	Mean	STD	Mean	STD	Mean	STD
16:0								
Liver								
PL	178	55	156	47	18	5	18	6
NL	833	101	686	35*	82	10	82	4
Total	1010	156	842	83				
Heart								
PL	78	22	43	10*	47	13	26	6*
NL	88	21	123	19	53	13	74	12
Total	166	44	166	30				
Brain								
PL	16	4	13	6	84	20	88	45
NL	3	2	2	1	16	9	12	4
Total	19	5	14	7				
20:4n-6								
Liver								
PL	310	64	276	35	39	8	38	5
NL	494	102	450	170	61	13	62	23
Total	804	166	727	205				
Heart								
PL	193	54	416	117*	51	14	61	17
NL	186	47	263	39	49	12	39	6
Total	379	101	679	156*				
Brain								
PL	24	7	22	4	92	26	94	15
NL	2	1	2	0.5	8	2	6	2
Total	26	7	24	4				
22:6n-3								
Liver								
PL	337	114	248	66	52	18	41	11
NL	307	145	355	132	48	22	59	22
Total	644	258	603	198				
Heart								
PL	227	28	116	36*	54	7	41	13
NL	195	50	168	11	46	12	59	4
Total	422	78	284	48*				
Brain								
PL	24	12	17	6	83	40	84	28
NL	5	2	3	2	17	6	16	9
Total	29	13	20	7				

Targeting of [1-^{14} C]16:0, [1-^{14}C]20:4n-6, or [1-^{14}C]22:6n-3 tracer to phospholipid (PL) and neutral lipid (NL) fractions into liver, heart, and brain. Values represent means ± SD (n = 3–4). The asterisk indicates a statistically significant difference from SW and C57BL/6 strains using a Student's unpaired, two-tailed t test ($p < 0.05$)

PL phospholipid pool, *NL* neutral lipid pool

Table 3 Targeting of fatty acid tracer into individual liver lipid classes in SW and C57BL/6 mice

	$k^* \times 10^{-5}$ (s^{-1})				Fractional dist. (%)			
	SW		C57BL/6		SW		C57BL/6	
	Mean	STD	Mean	STD	Mean	STD	Mean	STD
16:0								
TAG	785.2	89.90	650.4	31.1*	94.9	10.9	95.1	4.5
DAG	41.90	9.60	33.4	2.7	5.1	1.2	4.9	0.4
Ptd_2Gro	7.31	6.75	5.5	5.8	4.1	3.8	3.5	3.7
EtnGpl	27.16	9.31	19.96	9.12	15.3	5.2	12.8	5.9
PtdIns	3.45	2.18	1.84	0.84	1.9	1.2	1.2	0.5
PtdSer	1.68	0.52	1.36	0.77	0.9	0.3	0.9	0.5
ChoGpl	124.66	35.34	115.95	29.28	70.2	19.9	74.4	18.8
CerPCho	13.28	1.38	11.21	1.56	7.5	0.8	7.2	1.0
20:4n-6								
TAG	469.60	95.60	431.80	161.1	95.6	19.5	96.3	35.9
DAG	21.50	5.50	16.60	8.4	4.4	1.1	3.7	1.9
Ptd_2Gro	4.90	1.88	4.87	2.18	1.6	0.6	1.8	0.8
EtnGpl	29.34	5.06	36.14	1.98*	9.5	1.6	13.1	0.7*
PtdIns	15.07	5.97	14.23	4.11	4.9	1.9	5.2	1.5
PtdSer	5.73	1.56	5.71	1.39	1.9	0.5	2.1	0.5
ChoGpl	234.51	41.14	199.54	20.15	75.7	13.3	72.2	7.3
CerPCho	20.08	8.48	15.71	5.32	6.5	2.7	5.7	1.9
22:6n-3								
TAG	209.80	137.1	269.80	105.9	68.5	44.7	76.1	29.9
DAG	96.70	7.30	84.70	25.30	31.5	2.4	23.9	7.1
Ptd_2Gro	35.97	23.18	24.72	24.82	10.7	6.9	10.0	10.0
EtnGpl	143.04	47.67	123.17	7.06	42.4	14.1	49.6	2.8
PtdIns	16.04	6.17	10.09	3.64	4.8	1.8	4.1	1.5
PtdSer	14.09	5.19	10.00	5.89	4.2	1.5	4.0	2.4
ChoGpl	89.91	18.78	56.70	16.39	26.7	5.6	22.8	6.6
CerPCho	38.27	12.64	23.53	8.57	11.3	3.7	9.5	3.5

Esterification of [1-^{14} C]16:0, [1-^{14}C]20:4n-6, or [1-^{14}C]22:6n-3 into individual phospholipid and neutral lipid classes of liver tissue. Values represent means ± SD ($n = 3$–4). The asterisk indicates a statistically significant difference from SW and C57BL/6J strains using a Student's unpaired, two-tailed t test ($p < 0.05$)

In heart, esterification of [1-^{14}C]16:0 into ethanolamine glycerophospholipids (EtnGpl) and choline glycerophospholipids (ChoGpl) was reduced by 53 and 37 %, respectively (Table 4). A 51 % reduction in targeting of [1-^{14}C]16:0 into the diacylglycerol (DAG) fraction suggests a rapid esterification of DAG into TAG, which is consistent with the 1.5-fold increase in [1-^{14}C]16:0 targeting to TAG in C57BL/6 mice compared to SW mice (Table 4). Esterification of [1-^{14}C]20:4n-6 into heart was significantly increased in C57BL/6 mice. Increased targeting of [1-^{14}C]20:4n-6 into phospholipids is consistent with increased uptake into heart (Table 1) and into the phospholipid fraction (Table 2). Esterification of [1-^{14}C]20:4n-6 into all major phospholipids were significantly increased in heart of C57BL/6 mice; cardiolipin (Ptd_2Gro) 2.4-fold, EtnGpl 1.9-fold, phosphatidylinositol (PtdIns) 2.9-fold, phosphatidylserine (PtdSer) 3.6-fold, ChoGpl 2.1-fold, and sphingomyelin (CerPCho) 2.1-fold (Table 4). Esterification of [1-^{14}C]20:4n-6 into TAG was also increased 1.4-fold in heart of C57BL/6 mice (Table 4). In heart there was a significant decrease in esterification of [1-^{14}C]22:6n-3 into EtnGpl and ChoGpl, 44 and 52 % in C57BL/6 mice compared to SW mice, respectively, similar to that observed for 16:0 (Table 4).

There were no significant differences in esterification of [1-^{14}C]16:0 or [1-^{14}C]22:6n-3 into any brain lipid pools. However, esterification of [1-^{14}C]20:4n-6 into brain DAG pool was decreased 43 % in C57BL/6 mice compared to SW mice (Table 5).

Table 4 Targeting of fatty acid tracer into individual heart lipid classes in SW and C57BL/6 mice

	$k^* \times 10^{-5}$ (s^{-1})				Fractional dist. (%)			
	SW		C57BL/6		SW		C57BL/6	
	Mean	STD	Mean	STD	Mean	STD	Mean	STD
16:0								
TAG	73.84	18.08	113.76	13.57*	84.1	20.6	92.4	11.0
DAG	13.99	3.19	9.41	5.89	15.9	3.6	7.6	4.8*
Ptd_2Gro	2.26	0.56	1.36	1.06	2.9	0.7	3.2	2.5
EtnGpl	4.86	1.63	2.27	0.86*	6.2	2.1	5.3	2.0
PtdIns	0.94	0.70	0.40	0.35	1.2	0.9	0.9	0.8
PtdSer	0.55	0.88	0.28	0.22	0.7	1.1	0.7	0.5
ChoGpl	31.49	0.92	19.90	2.26*	40.2	1.2	46.6	5.3
CerPCho	38.17	17.48	18.49	5.40	48.8	22.3	43.3	12.6
20:4n-6								
TAG	168.65	42.45	241.50	32.62*	91.4	23.0	92.1	12.4
DAG	15.93	2.82	20.84	6.04	8.6	1.5	7.9	2.3
Ptd_2Gro	4.40	2.11	10.46	4.06*	2.3	1.1	2.5	1.0
EtnGpl	12.90	4.25	23.96	7.38*	6.7	2.2	5.8	1.8
PtdIns	9.78	4.94	28.23	7.98*	5.1	2.6	6.8	1.9
PtdSer	3.02	1.16	10.74	5.73*	1.6	0.6	2.6	1.4
ChoGpl	148.15	39.11	312.41	85.41*	76.8	20.3	75.1	20.5
CerPCho	14.55	2.40	30.05	6.07*	7.5	1.2	7.2	1.5
22:6n-3								
TAG	158.46	34.69	145.85	8.45	81.3	17.8	87.4	5.1
DAG	36.51	14.87	21.02	1.42	18.7	7.6	12.6	0.9
Ptd_2Gro	5.12	1.38	2.44	1.13	2.3	0.6	2.1	1.0
EtnGpl	37.89	4.20	21.19	3.94*	16.7	1.9	18.2	3.4
PtdIns	3.23	1.00	2.29	1.20	1.4	0.4	2.0	1.0
PtdSer	2.87	0.56	1.58	1.86	1.3	0.2	1.4	1.6
ChoGpl	159.52	19.18	76.98	22.79*	70.3	8.5	66.2	19.6
CerPCho	18.29	1.79	11.89	5.35	8.1	0.8	10.2	4.6

Esterification of [1-^{14} C]16:0, [1-^{14}C]20:4n-6, or [1-^{14}C]22:6n-3 into individual phospholipid and neutral lipid classes of heart tissue. Values represent means ± SD ($n = 3$–4). The asterisk indicates a statistically significant difference from SW and C57BL/6J strains using a Student's unpaired, two-tailed t test ($p < 0.05$)

Discussion

Although, resting metabolic rate and tissue turnover are not different between several strains of mouse [33], the impact of mouse strain on tissue fatty acid uptake and trafficking is poorly understood. Our results clearly indicate both similarities and differences in the uptake and trafficking of fatty acids into tissues of two commonly used mouse strains. Although there is a significant difference in fatty acid uptake and trafficking in heart between these two strains, surprisingly only minor differences were observed in brain and liver. Appreciating differences in characteristics between mouse strains to leverage the advantages and minimize potential pitfalls is an important consideration in experimental design [34]. For instance, C57BL/6 mice are commonly utilized in a substantial share of the scientific literature and are often used to study lipid metabolism, including studies on the efficacy of n-3 fatty acids on inflammation and injury [11, 12, 14, 35, 36]. On the other hand, SW mice are have been used in the pharmacology of fatty acid metabolism such as effects of pyridine exposure and high-fat diets on lipid metabolism [37–39]. Thus, we determined the differences in fatty acid uptake and trafficking in three tissues commonly used in experimental design using three fatty acids commonly found at the *sn*-1 position (16:0) and *sn*-2 position (20:4n-6 and 22:6n-3) of phospholipids.

Table 5 Targeting of fatty acid tracer into individual brain lipid classes in SW and C57BL/6 mice

	$k^* \times 10^{-5}$ (s^{-1})				Fractional dist. (%)			
	SW		C57BL/6		SW		C57BL/6	
	Mean	STD	Mean	STD	Mean	STD	Mean	STD
16:0								
TAG	1.24	0.81	0.81	0.34	42.5	27.7	47.2	19.8
DAG	1.68	0.80	0.91	0.21	57.5	27.4	52.8	12.5
Ptd_2Gro	0.05	0.08	0.18	0.36	0.7	1.1	3.1	6.1
EtnGpl	1.36	0.61	0.90	0.84	18.9	8.5	15.3	14.2
PtdIns	0.12	0.11	0.36	0.50	1.7	1.5	6.1	8.5
ChoGpl	5.68	0.20	4.46	1.26	78.8	2.8	75.6	21.4
20:4n-6								
TAG	0.50	0.27	0.62	0.04	24.1	13.1	41.1	2.6
DAG	1.57	0.30	0.89	0.45*	75.9	14.5	58.9	29.8
Ptd_2Gro	0.44	0.17	0.58	0.41	2.6	1.0	3.2	2.3
EtnGpl	1.99	0.73	1.87	0.30	11.9	4.4	10.4	1.7
PtdIns	6.67	0.75	6.31	0.57	39.8	4.5	35.1	3.2
ChoGpl	7.65	1.00	9.23	0.58	45.7	6.0	51.3	3.2
22:6n-3								
TAG	1.74	0.76	0.90	0.76	36.1	15.8	27.3	23.0
DAG	3.08	1.02	2.40	1.05	63.9	21.2	72.7	31.8
Ptd_2Gro	0.42	0.60	0.75	0.37	3.2	4.5	6.8	3.3
EtnGpl	6.03	1.96	5.53	1.26	45.4	14.7	50.0	11.4
PtdIns	1.17	0.76	0.49	0.40	8.8	5.7	4.4	3.6
ChoGpl	5.67	1.62	4.29	0.44	42.7	12.2	38.8	4.0

Esterification of [1-^{14} C]16:0, [1-^{14}C]20:4n-6, or [1-^{14}C]22:6n-3 into individual phospholipid and neutral lipid classes of brain tissue. Values represent means ± SD (n = 3–4). The asterisk indicates a statistically significant difference from SW and C57BL/6J strains using a Student's unpaired, two-tailed t test ($p < 0.05$)

In our study, one important observation is the differences between strains in the integrated plasma curve area in [1-^{14}C]20:4n-6 infused mice, but not for [1-^{14}C]16:0 and[1-^{14}C]22:6n-3. Such an observation using this steady-state kinetic model is not without precedence. In H-FABP (*Fabp3*) gene-ablated mice on a 129 × Balb/c background, there is a significant increase in average integrated plasma area of 16:0 in the gene-ablated mice, consistent with the profound reduction in 16:0 uptake into the heart [18] and presumably muscle tissue where H-FABP is also highly expressed [40, 41]. These data suggest that H-FABP can affect total body metabolism for fatty acids commonly used in β-oxidation, which is consistent with the reduced targeting of 16:0 into heart neutral lipids, e.g. TAG [18]. In rodents, 16:0 incorporation and turnover in TAG is very rapid indicating its use in β-oxidation [42]. Further, in rat lipid metabolism, 16:0, a saturated fatty acid, is mainly targeted towards β-oxidation [19, 43], whereas 20:4n-6 is mainly esterified into phospholipids [19], suggesting substantially different roles in the heart. Although we did not examine H-FABP levels between strains, the lack of change in the plasma curve for [1-^{14}C]16:0 does not suggest a difference in H-FABP levels as a potential mechanism, especially as the differences observed are for only 20:4n-6. However, a global change in 20:4n-6 metabolism, similar to that observed for 16:0 in H-FABP gene-ablated mice, may occur between mouse strains.

In C57BL/6 mice there is a homozygous disruption in the secretory group II phospholipase A_2 gene, while in CD-1:SW mice this is a heterozygous mutation when compared to several other normal genotype inbred mouse strains; including BALB/c, C3H/HE, DBA/1, DBA/2, NZB/B1N, and MRL *lpr*/*lpr* mice [15, 44]. This frameshift mutation occurs in the Ca^{2+} binding domain, rendering the group II $sPLA_2$ enzymatically inactive in C57BL/6 mice. The $sPLA_2$ family, I/II/V/X and otoconin-90, are closely related enzymes with a highly conserved Ca^{2+} binding loop that hydrolyze *sn*-2 fatty acids from phospholipids [45–47]. sPLA2 enzymes are vital in signal transduction as they often release 20:4n-6, which is enriched in the *sn*-2 position of phospholipids [48–50].

Although, group II $sPLA_2$ are *sn*-2 esterified fatty acid specific, they are not intrinsically 20:4n-6 specific [48, 51, 52]. Therefore, the preponderance of 20:4n-6 at

the *sn*-2 position may result in less fatty acid turnover in the C57BL/6 mice. We did not however, see a significant reduction of esterification into C57BL/6 mouse heart phospholipids in any of the fatty acids observed as one would expect due to the lack of specificity toward esterified fatty acids in group II $sPLA_2$. While the reduction in targeting of [1-^{14}C]16:0 and [1-^{14}C]22:6n-3 to EtnGpl and ChoGpl may be a result of reduced $sPLA_2$ activity, the lack of a reduction in 20:4n-6 incorporation into these mice suggest the decreased activity of $sPLA_2$ may not be critical for the changes observed between strains. However, in denervated rat heart, a reduction in general PLA_2 activity results in decreased 20:4n-6 turnover, which causes a reduction of 20:4n-6 incorporation into stable lipid compartments [42]. This is in contrast to our data as we observed a broad increase in esterification of 20:4n-6 into heart phospholipids in C57BL/6 mice, suggesting the difference in uptake and incorporation are not a result of this mutation in $sPLA_2$. However, because of the selective processes for the uptake of 20:4n-6 from plasma into heart phospholipids [19], we might have observed the significant increase in esterification into heart phospholipids due to increased 20:4n-6 availability in the plasma (Fig. 1). Therefore, changes in expression of some other gene may be altering uptake and/or metabolism of 20:4n-6, resulting in the observed differences between C57BL/6 and SW mice.

C57BL/6 mice are the most commonly used mouse strain to study metabolic diseases and they are one of the most susceptible to the development of diet-induced obesity and insulin resistance [53–55]. While insulin resistance is most associated with glucose intolerance, lipid metabolism is severely affected by this disease. Interestingly, when 129S6 mice are fed a high-fat diet there is increased obesity, hyperlipidemia, enhanced insulin secretion, glucose intolerance and fatty liver relative to control diet fed mice. However, BALB/c mice fed the same diet did not result in disease, but these mice had both enhanced insulin secretion and significantly improved glucose tolerance, suggesting insulin levels between strains can have a significant impact on phenotype [56]. Furthermore, when 129S6 are fed a high-fat diet, gene expression of acyl-CoA oxidase 1 (*Acox1*) is reduced, a protein which traffics fatty acids towards β-oxidation, however, under the same dietary conditions in BALB/C mice there is no change in expression [56]. Interestingly, in an *ex vivo* working heart model, C57BL/6 mice had increased *Acox1* expression as compared to 129/SvEvTac mouse heart, and as a result had decreased incorporation of oleic acid into TAG pools and more was utilized for β-oxidation than in 129/SvEvTac mouse heart [14]. Collectively, these studies demonstrate that observations in one mouse strain are not directly applicable to another strain, and support our supposition that for lipid metabolism, observations between mouse strains are not interchangeable.

Prior to this study, it was unknown what impact, if any, the strain of mouse had on tissue fatty acid uptake and trafficking into individual lipid classes. Hence, we report that two commonly used strains of mice had significant differences in heart fatty acid uptake and trafficking. While each of the fatty acids used were altered, the major effect was on the uptake and trafficking of 20:4n-6. This is important as 20:4n-6 is an important signaling molecule in the heart [57–61]. This is an important consideration because there is an enormous body of literature in which these mouse strains have been used interchangeably. Our data suggest that investigators must be careful when comparing results involving lipid metabolism between these strains and this is more likely applicable for studies involving lipid metabolism between different mouse strains in general.

Acknowledgments We thank Dr. Carole Haselton for excellent surgical and technical skills that contributed to this work. This work was supported by a grant to EJM by the American Heart Association (0151121Z).

Compliance with Ethical Standards

Conflict of interest The authors declare no conflict of interest.

References

1. Goren HJ, Kulkarni RN, Kahn CR (2004) Glucose homeostasis and tissue transcript content of insulin signaling intermediates in four inbred strains of mice: C57BL/6, C57BLKS/6, DBA/2, and 129X1. Endocrinology 145:3307–3323
2. Berglund E, Li C, Poffenberger G, Ayala J (2008) Glucose metabolism in vivo in four commonly used inbred mouse strains. Diabetes 57:1790–1799
3. Andrikopoulos S, Massa CM, Aston-Mourney K, Funkat A, Fam BC, Hull RL, Kahn SE, Proietto J (2005) Differential effect of inbred mouse strain (C57BL/6, DBA/2, 129T2) on insulin secretory function in response to a high fat diet. J Endocrinol 187:45–53
4. Haramizu S, Nagasawa A, Ota N, Hase T, Tokimitsu I, Murase T (2009) Different contribution of muscle and liver lipid metabolism to endurance capacity and obesity susceptibility of mice. J Appl Physiol 106:871–879
5. Montgomery MK, Hallahan NL, Brown SH, Liu M, Mitchell TW, Cooney GJ, Turner N (2013) Mouse strain-dependent variation in obesity and glucose homeostasis in response to high-fat feeding. Diabetologia 56:1129–1139
6. Rendina-Ruedy E, Hembree KD, Sasaki A, Davis MR, Lightfoot SA, Clarke SL, Lucas EA, Smith BJ (2015) A comparative study of the metabolic and skeletal response of C57BL/6J and C57BL/6N mice in a diet-induced model of type 2 diabetes. J Nutr Metab 2015:1–13
7. Haluzik M, Colombo C, Gavrilova O, Chua S, Wolf N, Chen M, Stannard B, Dietz KR, Le Roith D, Reitman ML (2004) Genetic background (C57BL/6J versus FVB/N) strongly influences the severity of diabetes and insulin resistance in ob/ob mice. Endocrinology 145:3258–3264

8. Mekada K, Abe K, Murakami A, Nakamura S, Nakata H, Moriwaki K, Obata Y, Yoshiki A (2009) Genetic differences among C57BL/6 substrains. Exp Anim 58:141–149
9. Simpson EM, Linder CC, Sargent EE, Davisson MT, Mobraaten LE, Sharp JJ (1997) Genetic variation among 129 substrains and its importance for targeted mutagenesis in mice. Nat Genet 16:19–27
10. Myers-Payne SC, Hubbell T, Pu L, Schnütgen F, Börchers T, Wood WG, Spener F, Schroeder F (1996) Isolation and characterization of two fatty acid binding proteins from mouse brain. J Neurochem 66:1648–1656
11. Balogun KA, Albert CJ, Ford DA, Brown RJ, Cheema SK (2013) Dietary omega-3 polyunsaturated fatty acids alter the fatty acid composition of hepatic and plasma bioactive lipids in C57BL/6 mice: a lipidomic approach. PLoS One 8:1–16
12. Zhang M, Wang S, Mao L, Leak RK, Shi Y, Zhang W, Hu X, Sun B, Cao G, Gao Y, Xu Y, Chen J, Zhang F (2014) Omega-3 fatty acids protect the brain against ischemic injury by activating Nrf2 and upregulating heme oxygenase 1. J Neurosci 34:1903–1915
13. Lim SN, Gladman SJ, Dyall SC, Patel U, Virani N, Kang JX, Priestley JV, Michael-Titus AT (2013) Transgenic mice with high endogenous omega-3 fatty acids are protected from spinal cord injury. Neurobiol Dis 51:104–112
14. Vaillant F, Lauzier B, Poirier I, Gélinas R, Rivard M-E, Robillard Frayne I, Thorin E, Des Rosiers C (2014) Mouse strain differences in metabolic fluxes and function of ex vivo working hearts. Am J Physiol Heart Circ Physiol 306:H78–H87
15. Kennedy BP, Payette P, Mudgett J, Vadas P, Pruzanski W, Kwan M, Tang C, Rancourt DE, Cromlish WA (1995) A natural disruption of the secretory group II phospholipase A2 gene in inbred mouse strains. J Biol Chem 270:22378–22385
16. Robinson PJ, Noronha J, DeGeorge JJ, Freed LM, Nariai T, Rapoport SI (1992) A quantitative method for measuring regional in vivo fatty-acid incorporation into and turnover within brain phospholipids: review and critical analysis. Brain Res Brain Res Rev 17:187–214
17. Golovko MY, Faergeman NJ, Cole NB, Castagnet PI, Nussbaum RL, Murphy EJ (2005) Alpha-synuclein gene deletion decreases brain palmitate uptake and alters the palmitate metabolism in the absence of alpha-synuclein palmitate binding. Biochemistry 44:8251–8259
18. Murphy EJ, Barcelo-Coblijn G, Binas B, Glatz JFC (2004) Heart fatty acid uptake is decreased in heart fatty acid-binding protein gene-ablated mice. J Biol Chem 279:34481–34488
19. Murphy EJ, Rosenberger TA, Patrick CB, Rapoport SI (2000) Intravenously injected [1-14C]arachidonic acid targets phospholipids, and [1-14C]palmitic acid targets neutral lipids in hearts of awake rats. Lipids 35:891–898
20. Murphy EJ (2010) Brain fixation for analysis of brain lipid-mediators of signal transduction and brain eicosanoids requires head-focused microwave irradiation: an historical perspective. Prostaglandins Other Lipid Mediat 91:63–67
21. Folch J, Lees M, Sloane Stanley G (1957) A simple method for the isolation and purification of total lipides from animal tissues. J Biol Chem 226:497–509
22. Murphy CC, Murphy EJ, Golovko MY (2008) Erucic acid is differentially taken up and metabolized in rat liver and heart. Lipids 43:391–400
23. Smith BS (1970) A comparison of 125-I and 51-Cr for measurement of total blood volume and residual blood content of tissues in the rat; evidence for accumulation of 51-Cr by tissues. Clin Chim Acta 27:105–108
24. Regoeczi E, Taylor P (1978) The net weight of the rat liver. Growth 42:451–456
25. Rosenberger TA, Oki J, Purdon AD, Rapoport SI, Murphy EJ (2002) Rapid synthesis and turnover of brain microsomal ether phospholipids in the adult rat. J Lipid Res 43:59–68
26. Rosenberger TA, Villacreses NE, Contreras MA, Bonventre JV, Rapoport SI (2003) Brain lipid metabolism in the cPLA2 knockout mouse. J Lipid Res 44:109–117
27. Marcheselli BL, Scott VL, Reddy TS, Bazan NG (1988) Quantitative analysis of acyl group composition of brain phospholipids, neutral lipids, and free fatty acids. In: Boulton AA, Baker GB, Horrocks LA (eds) Lipids and Related Compouinds, Neuromethods, vol 7. Humana Press, Clifton, NJ, pp 83–110
28. Jolly CA, Hubbell T, Behnke WD, Schroeder F (1997) Fatty acid binding protein: stimulation of microsomal phosphatidic acid formation. Arch Biochem Biophys 341:112–121
29. Bradford MM (1976) A rapid and sensitive method for the quantitation of microgram quantities of protein utilizing the principle of protein-dye binding. Anal Biochem 72:248–254
30. Murphy EJ, Horrocks LA (1993) A model for compression trauma: pressure-induced injury in cell cultures. J Neurotrauma 10:431–444
31. Gnaedinger JM, Miller JC, Latker CH, Rapoport SI (1988) Cerebral metabolism of plasma [14C]palmitate in awake, adult rat: subcellular localization. Neurochem Res 13:21–29
32. Miller JC, Gnaedinger JM, Rapoport SI (1987) Utilization of plasma fatty acid in rat brain: distribution of [14C]palmitate between oxidative and synthetic pathways. J Neurochem 49:1507–1514
33. MacAvoy SE, Lazaroff S, Kraeer K, Arneson LS (2012) Sex and strain differences in isotope turnover rates and metabolism in house mice (*Mus musculus*). Can J Zool Can Zool 90:984–990
34. Chia R, Achilli F, Festing MFW, Fisher EMC (2005) The origins and uses of mouse outbred stocks. Nat Genet 37:1181–1186
35. Jolly CA, Jiang YH, Chapkin RS, McMurray DN (1997) Dietary (n-3) polyunsaturated fatty acids suppress murine lymphoproliferation, interleukin-2 secretion, and the formation of diacylglycerol and ceramide. J Nutr 127:37–43
36. Zimring JC, Smith N, Stowell SR, Johnsen JM, Bell LN, Francis RO, Hod EA, Hendrickson JE, Roback JD, Spitalnik SL (2014) Strain-specific red blood cell storage, metabolism, and eicosanoid generation in a mouse model. Transfusion 54:137–148
37. Wheelock CE, Forshed J, Goto S, Hammock BD, Newman JW (2008) Effects of pyridine exposure upon structural lipid metabolism in Swiss Webster mice. Chem Res Toxicol 21:583–590
38. Liu Z, Lim CY, Su MYF, Soh SLY, Shui G, Wenk MR, Grove KL, Radda GK, Han W, Xiao X (2013) Neonatal overnutrition in mice exacerbates high-fat diet-induced metabolic perturbations. J Endocrinol 219:131–143
39. Glavas MM, Kirigiti MA, Xiao XQ, Enriori PJ, Fisher SK, Evans AE, Grayson BE, Cowley MA, Smith MS, Grove KL (2010) Early overnutrition results in early-onset arcuate leptin resistance and increased sensitivity to high-fat diet. Endocrinology 151:1598–1610
40. Glatz JF, van der Vusse GJ (1989) Intracellular transport of lipids. Mol Cell Biochem 88:37–44
41. Zschiesche W, Kleine AH, Spitzer E, Veerkamp JH, Glatz JF (1995) Histochemical localization of heart-type fatty-acid binding protein in human and murine tissues. Histochem Cell Biol 103:147–156
42. Patrick CB, McHowat J, Rosenberger TA, Rapoport SI, Murphy EJ (2005) Arachidonic acid incorporation and turnover is decreased in sympathetically denervated rat heart. Am J Physiol Heart Circ Physiol 288:H2611–H2619
43. Degrella RF, Light RJ (1980) Uptake and metabolism of fatty acids by dispersed adult rat heart myocytes. J Biol Chem 255:9731–9738
44. MacPhee M, Chepenik KP, Liddell RA, Nelson KK, Siracusa LD, Buchberg AM (1995) The secretory phospholipase A2 gene is a candidate for the Mom1 locus, a major modifier of ApcMin-induced intestinal neoplasia. Cell 81:957–966

45. Lambeau G, Ancian P, Nicolas J-P, Beiboer SHW, Moinier D, Verheij H, Lazdunski M (1995) Structural elements of secretory phospholipases A2 involved in the binding to M-type receptors. J Biol Chem 270:5534–5540
46. Fukagawa T, Nose T, Shimohigashi Y, Ogawa T, Oda N, Nakashima K, Chang CC, Ohno M (1993) Purification, sequencing and characterization of single amino acid-substituted phospholipase A2 isozymes from *Trimeresurus gramineus* (green habu snake) venom. Toxicon 31:957–967
47. Six DA, Dennis EA (2000) The expanding superfamily of phospholipase A2 enzymes: classification and characterization. Biochim Biophys Acta Mol Cell Biol Lipids 1488:1–19
48. Murakami M, Kudo I (2002) Phospholipase A2. J Biochem 131:285–292
49. Mounier CM, Ghomashchi F, Lindsay MR, James S, Singer AG, Parton RG, Gelb MH (2004) Arachidonic acid release from mammalian cells transfected with human groups IIA and X secreted phospholipase A2 occurs predominantly during the secretory process and with the involvement of cytosolic phospholipase A2-α. J Biol Chem 279:25024–25038
50. Murakami M, Taketomi Y, Sato H, Yamamoto K (2011) Secreted phospholipase A2 revisited. J Biochem 150:233–255
51. With C, Phospholipase C, Murakami M, Shimbara S, Kambe T, Kuwata H, Winstead MV, Tischfield JA, Kudo I (1998) The functions of five distinct mammalian phospholipase A 2s in regulating arachidonic acid release. Biochemistry 273:14411–14423
52. Singer AG, Ghomashchi F, Le Calvez C, Bollinger J, Bezzine S, Rouault M, Sadilek M, Nguyen E, Lazdunski M, Lambeau G, Gelb MH (2002) Interfacial kinetic and binding properties of the complete set of human and mouse groups I, II, V, X, and XII secreted phospholipases A2. J Biol Chem 277:48535–48549
53. Surwit RS, Kuhn CM, Cochrane C, McCubbin JA, Feinglos MN (1988) Diet-induced type II diabetes in C57BL/6J mice. Diabetes 37:1163–1167
54. Black BL, Croom J, Eisen EJ, Petro AE, Edwards CL, Surwit RS (1998) Differential effects of fat and sucrose on body composition in A/J and C57BL/6 mice. Metabolism 47:1354–1359
55. Toye AA, Lippiat JD, Proks P, Shimomura K, Bentley L, Hugill A, Mijat V, Goldsworthy M, Moir L, Haynes A, Quarterman J, Freeman HC, Ashcroft FM, Cox RD (2005) A genetic and physiological study of impaired glucose homeostasis control in C57BL/6J mice. Diabetologia 48:675–686
56. Toye AA, Dumas ME, Blancher C, Rothwell AR, Fearnside JF, Wilder SP, Bihoreau MT, Cloarec O, Azzouzi I, Young S, Barton RH, Holmes E, McCarthy MI, Tatoud R, Nicholson JK, Scott J, Gauguier D (2007) Subtle metabolic and liver gene transcriptional changes underlie diet-induced fatty liver susceptibility in insulin-resistant mice. Diabetologia 50:1867–1879
57. Liu SJ, McHowat J (1998) Stimulation of different phospholipase A2 isoforms by TNF-alpha and IL-1beta in adult rat ventricular myocytes. Am J Physiol 275:H1462–H1472
58. McHowat J, Liu S (1997) Interleukin-1beta stimulates phospholipase A2 activity in adult rat ventricular myocytes. Am J Physiol 272:C450–C456
59. McHowat J, Creer MH (2001) Comparative roles of phospholipase A2 isoforms in cardiovascular pathophysiology. Cardiovasc Toxicol 1:253–265
60. Steer SA, Wirsig KC, Creer MH, Ford DA, McHowat J (2002) Regulation of membrane-associated iPLA2 activity by a novel PKC isoform in ventricular myocytes. Am J Physiol Cell Physiol 283:C1621–C1626
61. Pavoine C, Magne S, Sauvadet A, Pecker F (1999) Evidence for a beta2-adrenergic/arachidonic acid pathway in ventricular cardiomyocytes. Regulation by the beta1-adrenergic/camp pathway. J Biol Chem 274:628–637